Mineralogical and chemical variations of the lunar crust: Results from radiative transfer modeling of central peaks. L. Z. Sun[1], Z. C. Ling[1,2], J. Zhang[1], J. Chen[1], Z. J. Li[1], J. Z. Liu[3]. [1] Shandong Provincial Key Laboratory of Optical Astronomy & Solar-Terrestrial Environment, Institute of Space Sciences, Shandong University, Weihai 264209, China (sunlz9008@gmail.com), [2] Key Laboratory of Lunar and Deep Space Exploration, Chinese Academy of Sciences, Beijing 100012, China, [3] Institute of Geochemistry, Chinese Academy of Sciences, Guiyang, 550002, China.

Introduction: Remote sensing studies can present a global view of the mineralogical and compositional distributions for the Moon. Lunar crater central peaks are supposed to have exhumed crustal material beneath the surface, giving us an opportunity to survey the compositional distributions in the crust at depth [1,2].

In this study, in order to explore the compositional abundances and distributions within the lunar crust, we investigated the mineral abundances of 89 lunar central peaks by applying an improved Hapke radiative transfer model to spectral data from Moon Mineralogy Mapper (M^3).

Methods: Supposing a medium filled with closely packed particles, and the grain size of these particles are larger than wavelengths, then the reflectance of this medium can be described with radiative transfer theory [3-5]. Here, we introduce a new radiative transfer model that consider both the chemical compositions (e.g., Mg', Fo, Fs, Wo) and space weathering effect (Figure 1). The radiative transfer function used in this study is expressed as Eq. (1), which takes lunar soil porosity and shadow-hiding opposition effect (SHOE) into consideration [4,6].

$$R(\mathrm{i},\mathrm{e},\mathrm{g}) = K\frac{\omega}{4\pi}\frac{\mu_0}{\mu_0+\mu}\{p(\mathrm{g})[1+\mathrm{B}_s(\mathrm{g})]+[\mathrm{H}(\mu_0/K)\,\mathrm{H}(\mu/K)-1]\} \quad (1)$$

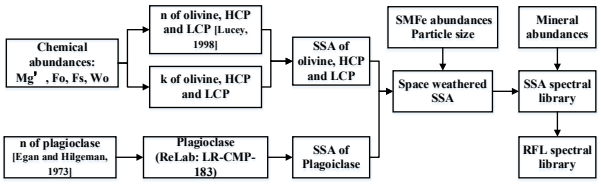

Figure 1. Flow chart of spectral library building process.

Here R refers to reflectance and ω refers to single scattering albedo (SSA). *i, e*, and *g* are the incident, emergence and phase angles respectively. In this paper, i = e = g/2 = π/6. $\mu_0 / (\mu_0 + \mu)$ is the *Lommel-Seeliger* parameter, where $\mu_0 = cos(i)$ *and* $\mu = cos(e)$ [5]. K is the porosity factor, it increases as the particles of a medium are compacted. $P(g)$ is the phase function, $B_s(g)$ mainly describes the shadow-hiding opposition effect (SHOE) [4], which also refers to shadow-hiding backscattering effect. Using the algorithm described in Figure 1, we finally build a spectral library containing more than 10 million spectra.

Results and discussion: We derive the mineral abundances of 89 central peaks based on radiative transfer modeling and an advanced spectral matching method (Figure 2). For global mineral abundances analysis, we average the mineral abundances for each central peak to better understand their distributions. Global averaged mineral content (range) of 89 central peaks are: plagioclase, 92% (55.1–100%); LCP, 5.1% (0–22.9%); Olivine, 1.5% (0–17.3%); HCP, 1.4% (0–10.4%). This result indicate a very anorthositic crustal composition.FHT is most abundant in Plagioclase, and FHT-O is a little more mafic than FHT-A. Mafic minerals are mainly distributed close to impact basins (like Imbrium, Procellarum and SPA). Olivine shows a decentralized distribution in the lunar crust and only concentrated in several craters, like Copernicus and Eratosthenes crater in PKT, White crater in SPAT and some other craters located near large impact basins in FHT-O. HCP is the least abundant mineral and primarily confined to SPAT. LCP is the most abundant mafic mineral and is widespread in the lunar crust. SPAT has the highest LCP concentration (~13.4% on average), followed by PKT (~5.9% on average).

We analyze the variation of average mineral abundances and chemical compositions of 89 central peaks from 5 terranes relative to their mantle distance (=lunar crustal thickness – crater excavation depth) (Figure 3). We used lunar crustal thickness data from GRAIL [7] and crater excavation depth from Lunar Impact Crater Database [8,9] to calculated the mantle distance for each central peak. The distances between central peaks origin and crust-mantle interface are ~15–51 km for FHT, ~14–29 km for PKT and ~2-31 km for SPAT. If we take all the lunar terranes as a whole, it can be seen from Figure 3 that plagioclase content increases with mantle distance, and the abundances of olivine, HCP and LCP decrease with mantle distance. However, if each terrane is examined separately, a similar trend can only be observed in FHT (including FHT-O and FHT-A). Olivine and HCP have very low abundances in the crust and very few exposures in the central peaks, for instance, olivine only concentrates in a few central peaks and HCP-rich central peaks are largely confined to SPAT. Plagioclase and LCP are both abundant and widespread in the crust comparing to olivine and HCP, making it possible to examine their variation trend in each terrane. Plagioclase in FHT is highly abundant (>80%) and increases slowly with mantle distance; while in PKT and SPAT (including SPAT and SPAT-O),

plagioclase contents are lower and increase faster with depth (Figure 3a). Meanwhile, LCP content in FHT is low and decreases slowly with mantle distance in the crust; LCP abundances in PKT and SPAT are more abundant and decrease faster than FHT. The abundance and variation trend of central peak minerals in FHT deviate from PKT and SPAT. We conclude that the mafic/plagioclase ratio increases depth and the rate of increase grows with depth in the lunar crust.

Mg' is derived for central peaks that contains mafic minerals, and its global averaged value is ~74 (42–80). Fo is derived for olivine mineral, and it's global averaged value is ~71 (40–80). The vertical variations of Mg' and Fo for each terrane are shown in Figure 4. Globally, Mg' and Fo gradually decrease as the distance to mantle increases. In FHT, Mg' and Fo span a wide range from ~42 to 80, and no asymmetry can be observed between the Mg' distributions in FHT-A and FHT-O. Mg' and Fo in PKT have a very disperse distribution, mostly concentrated in the high end, with only two or three craters show ferroan compositions. No asymmetry in Mg' between FHT-A and PKT is observed, either. Craters in SPAT are highly magnesian, and their Mg' and Fo are around 80.

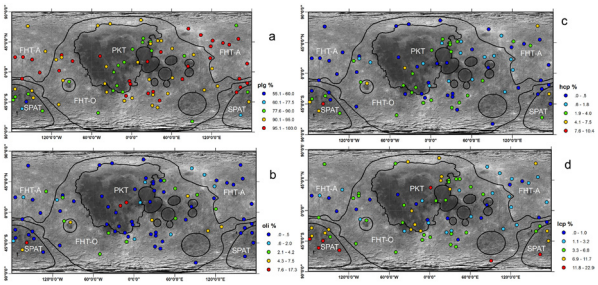

Figure 2. The location of 89 central peaks and their average mineral abundances plotted on Clementine 750 nm base map. From top to bottom are (a) plagioclase, (b) olivine, (c) HCP and (d) LCP. Solid lines indicate approximate lunar terrane boundaries [10].

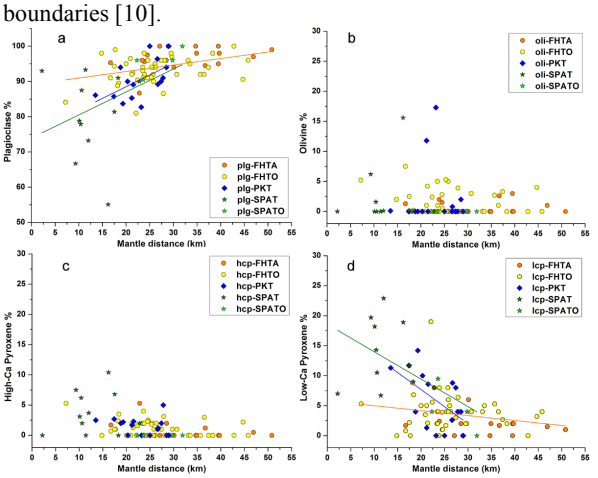

Figure 3. Average abundance of (a) plagioclase, (b) olivine, (c) High-Ca Pyroxene (HCP) and (d) Low-Ca Pyroxene (LCP) versus the proximity to lunar crust-mantle boundary (mantle distance). Solid lines in figure (a) and (d) that colored in orange, green and blue are the linear fitted lines for FHT (including FHT-A and FHT-O), PKT and SPAT (including SPAT and SPAT-O).

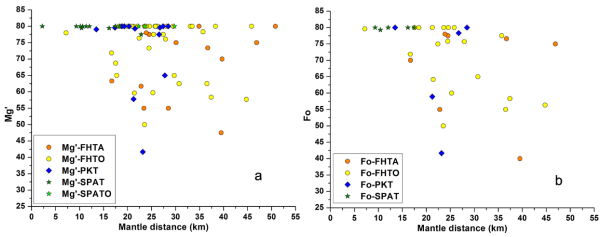

Figure 4. (a) Average Mg' for mafic minerals; (b) average Fo for olivine mineral, and no olivine is detected in SPAT-O.

Conclusions: 1) The lunar "pristine" crustal rocks are rich in plagioclase, and their mafic minerals are dominated by low-Ca pyroxene and olivine [11]. Therefore, the major rock types are anorthosite, nortite, troctolite, and slight gabbro [11,12]. The mineral modes analyzed from 89 central peaks by this work suggest lunar crust is highly anorthositc (>90% plagioclase), and major rock types are anorthosite, noritic anorthosite and troctolite anorthosite (except SPAT). Mafic minerals are dominated by LCP, followed by olivine and a few HCP. Therefore, our work shows a coherent composition with pristine crustal samples. 2) Plagioclase is both abundant and widespread all over the crust, suggesting a massive residual of the primordial feldspathic crust may still exist in the Moon. 3) The mafic/plagioclase ratio increases with depth in the crust, and the rate of increase grows with depth. 4) No asymmetry of Mg' is observed between central peaks from nearside and farside.

References: [1] Tompkins S., Pieters C. M. (1999) *Meteoritics & Planet. Sci., 34*, 25-41. [2] Melosh H. J. (1989),Impact Cratering: A Geologic Process. New York: Oxford University Press. [3] Hapke B. (2001) *JGR, 106*, 10039-10073. [4] Hapke B. (2012),Theory of reflectance and emittance spectroscopy: Cambridge University Press. [5] Hapke B. (1981) *JGR, 86*, 3039-3054. [6] Hapke B. (1986) *Icarus, 67*, 264-280. [7] Wieczorek M. A., et al. (2013) *Science, 339*, 671-675. [8] Losiak A., et al. (2009) *LPS XL,* Abstract # 1532. [9] Stöffler D., et al. (2006) *Rev. Mineral. Geochem., 60*, 519-596. [10] Jolliff B. L., et al. (2000) *JGR, 105*, 4197-4216. [11] Wieczorek M. A., et al. (2006) *Rev. Mineral. Geochem., 60*, 221-364. [12] Papike J. J., et al. (1998) *Rev. Mineral. Geochem., 36*, 5.1-5.234.